proceedings

MDPI

Proceeding

Evaluation of fracture process in concrete by means of acoustic approaches†

Tomoki Shiotani [1]*, Hisafumi Asaue[1], Katsufumi Hashimoto[1], Takahiro Nisahida[1]

[1] Dept. Civil & Earth Resources Engineering, Graduate School of Engineering, Kyoto University, 615-8540 Kyoto, Japan

Emails: shiotani.tomoki.2v@kyoto-u.ac.jp; asaue.hisafumi.7a@kyoto-u.ac.jp; hashimoto.katsufumi.8a@kyoto-u.ac.jp; nishida.takahiro.6e@kyoto-u.ac.jp

* Correspondence: shiotani.tomoki.2v@kyoto-u.ac.jp; Tel.: +81-75-383-3494

† Presented at the 18th International Conference on Experimental Mechanics, ICEM18, Brussels, 2018

Published:

Abstract: Through the life cycle of civil infrastructures, quality assessments shall be implemented when construction, in-service, before/ after repair and so forth; however, there are no decisive techniques to evaluate inside of structures non-destructively. The authors have developed an advanced measurement method using tomographic approaches. With these advanced technologies, internal damage or defects can be visualized as a distribution of elastic wave parameters such as velocities so that damage identification consisting of locations and damage degree would be possible. In the paper, fracture processes of concrete decks are visualized by the acoustic approaches. Specifically, RC slabs with/ without water supply subject to wheel loads are cyclically damaged with monitoring acoustic approaches. As a result, depending on the water condition, different pattern of fracture progress can be confirmed.

Keywords: Concrete; wheel loads; acoustic approaches; fatigue failure; fracture process

1. Introduction

As road infrastructures have been constructed intensively since 1960s, almost those are reaching their life-span 50 years recently in Japan. Accordingly ageing rate of more than 50 years old shifted to 43% in coming 10 years from 18% of 2013 [1]. Replacement of those ageing infrastructures with new ones would be the most ideal measure; however, due to shrinkage of taxation, leading decrease of construction budget, life-prolonging tactics are appeared to be the most adaptable for those existing ageing infrastructures. While for new structures, proactive maintenance from the early damage phase is widely recognized as the most cost-effective life cycle scenario; however, as not only for detective techniques for the early damage but also for corresponding repair methods, those have yet to be developed, substantial proactive maintenance treatment has not so far been applied for the new infrastructures. Among the infrastructures, concrete bridge decks hold many difficult problems, resulting in taking a lot of cost to maintain. Specifically, it is planned by three major expressway companies that more than 90% of the renewal budget for 15 years will be used for bridge decks. The RC bridge decks are so principal members of road infrastructures to maintain that many organizations have studied intensively for their deterioration mechanisms, countermeasures against deterioration, and so forth. In order to simulate the peculiar failure process of the bridge decks experimentally, test slabs have been subjected to wheel loading tests with NDT approaches [2, 3]. A three-dimensional approach using AE tomography [4, 5] have been applied recently, and fatigue failure mechanisms could be explained by a velocity distribution of elastic waves [6]. In addition, data assimilation using resultant wave velocities have been conducted, and remaining life time could be successfully estimated by Path-Integral-Mechanistic Model [7l. In this paper, comparison is made

between fatigue failure mechanisms with and without water supply by acoustic approaches. Final form of deterioration specified in RC decks namely 'aggregation' is discussed by the findings. Note 'aggregation' is the final form of deterioration of RC decks, remaining only aggregate from concrete where cement hydrated matrix is washed out by excessive water pressures filled in the cracks due to mobile loads.

2. Measurement and acoustic monitoring approaches

In order to simulate cracks actually observed in the slabs due to fatigue, repeated loading with a steel wheel was conducted. As shown in Fig. 1, a foundation put on the slab is cyclically moved in a lateral direction, which is different from the wheel-loading apparatus installed movable loading-wheel [3]. In the apparatus, a steel wheel of 300 mm in diameter and 400 mm in width can be loaded up to 250 kN in the case of repeated lateral loading and 534 kN in the case of static vertical loading. The foundation can move horizontally from ±500 mm to ±1000 mm. In the experiment, the motion of ±500 mm and the repeated rate 8.97 rpm were applied. Here, step-wise cyclic loadings are employed as shown in Fig. 1. In the first steps, the load of 98 kN was repeatedly applied up to 100k times. In the second steps, the load of 127.4 kN were applied up to 200k times. Then, the third step loadings were conducted until 250k times with 156.8 kN load where the fatigue limit of the specimen was estimated as 235×k times.

A slab specimen is made of reinforced concrete with rebar arrangement (detail can be found in Ref. 6). The specimen is a plate of dimensions 3000 ×2000 ×210 mm. Mixture proportions of concrete is indicated in Table 1. The strength was 20.7 N/mm^2. In case of water supply, a central area of the top surface (see the bold blue rectangle in Fig. 2) is kept saturated by continuous water supplying to a certain height. 31 strain gauges for the vertical direction are embedded in the specimen.

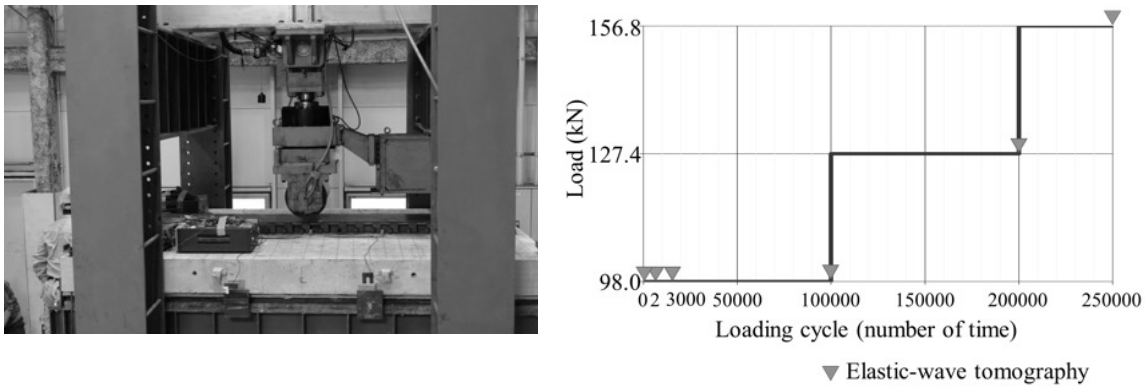

Figure 1. Wheel loading apparatus (left) and load application program (right).

Table 1. Mixture proportion of concrete slab.

Max. gravel size (mm)	Slump (cm)	W/C (%)	Volume ratio of sand s/a (%)	Air (%)	Unit weight per 1 m^3 concrete (kg/m^3)				
					Water: W	Cement: C	Sand: S	Gravel: G	Admixture
20	12	64.3	46.6	4.5	178	277	839	1055	2.27

Arrangement of AE sensors and excitation locations are demonstrated as in Fig. 2. 36 AE sensors of 60 kHz resonance are arranged onto the specimen, namely 10 for top, 18 for bottom and 8 for sides. For elastic wave tomography, excitations are made by a 35 mm dia. steel ball for 18 points on the top as to avoid the loading area depicted by a green broken rectangle, and 28 points on the bottom. Measurement of elastic wave excitations are conducted six times: before loading, after second, after 3k, after 100k, after 200k load applications, and after failure. Detected signals by the sensors are amplified by 40 dB at preamplifier and acquired by the monitoring system of 48-channel Express-8 (Physical Acoustics Corp) with a 1 MHz sampling rate. 17 displacement-meters are set at the bottom. Seven electric strain gauges for detecting the vertical deformation are embedded inside the concrete.

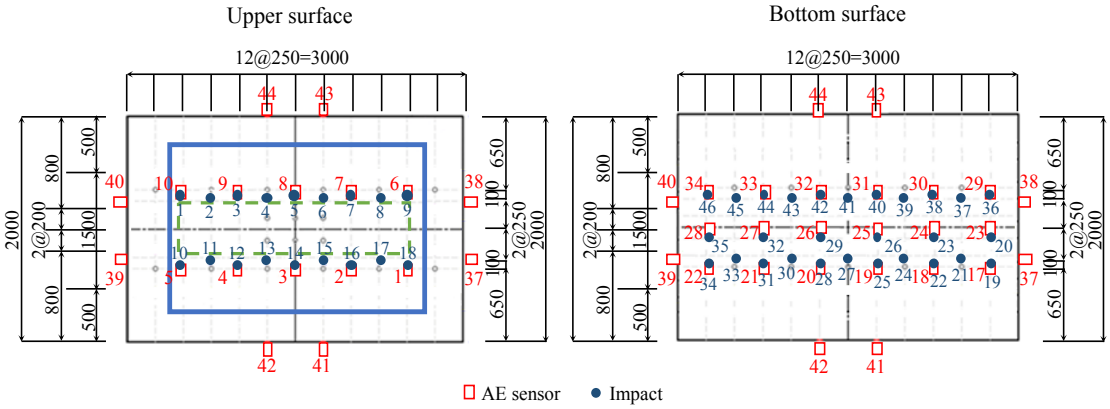

Figure 2. Locations of AE sensors and excitation points denoted by red squares and blue circles, respectively.

Elastic wave tomography [8] and AE tomography [4, 5] are methods for addressing the deterioration with elastic wave parameters such as velocity are obtained based on the following wave sources. In the elastic wave tomography, the source location and excitation time are both known whereas both unknown for AE tomography. Specifically, the tomography evaluates concrete characteristics using some peculiar elastic wave features in each set-element over the structure based on variations of elastic waves parameters through the propagation e.g., velocity, frequency, amplitude, and so forth. Among the parameters, the elastic wave velocity can be linked to the modulus of elasticity which itself varies depending on the presence of internal damages such as cracks or voids. In detail under the existence of such defects as voids or cracks, the elastic waves result in exhibition behaving scattering, reflection and diffraction, leading to the decrease of elastic wave velocity. Then it can reasonably be assumed that a small elastic wave velocity means a higher level of deterioration. Accordingly, the wave velocity can be a good indicator of the internal condition of concrete structures so that it has thus been well used to evaluate the deterioration.

3. Results and discussions

3.1 Dry condition

The analysis of 3D tomography was conducted in the region of 3000 × 1000 × 210 mm of the slab, which consists of 25 nodes in the axial direction, 13 nodes in the lateral direction and 5 nodes in the thickness direction. Totally the velocities of 1152 elements were obtained by means of elastic wave tomography.

Contour maps on distributions of the velocities are shown in Fig. 3. Prior to the experiment, the velocity zones of approximately 3500 m/s are widely observed and relatively-low velocity zone (about 3000 to 3500 m/s) is identified in a lattice pattern. This lattice pattern might be attributed to the sensor cables arrangements in concrete slab [6]. After 2 cycles loading, the relatively-low velocity area toward the center of slab, which might represent the punching-shear damage of concrete slab due to wheel loading as shown in Fig. 4, appears on behalf of the lattice pattern. The situations are still similar after 3k, and 100k cycles. However, after 200k cycles, the zones of the velocities lower than 2700 m/s is identified at 2.3 m distance in the axial direction. After 250k cycles, which exhibits cycles beyond the fatigue limit, the zones of the velocities lower than 2500 m/s widely spread over the concrete slab. From Fig. 3, the trends of the decrease in the velocities are dominant after 250k cycles. It is found that the velocity distributions show minor variations up to 100k cycles, while generation of low-velocity zones is initiated after 200k cycles, leading to the fatigue limit before 250k cycles.

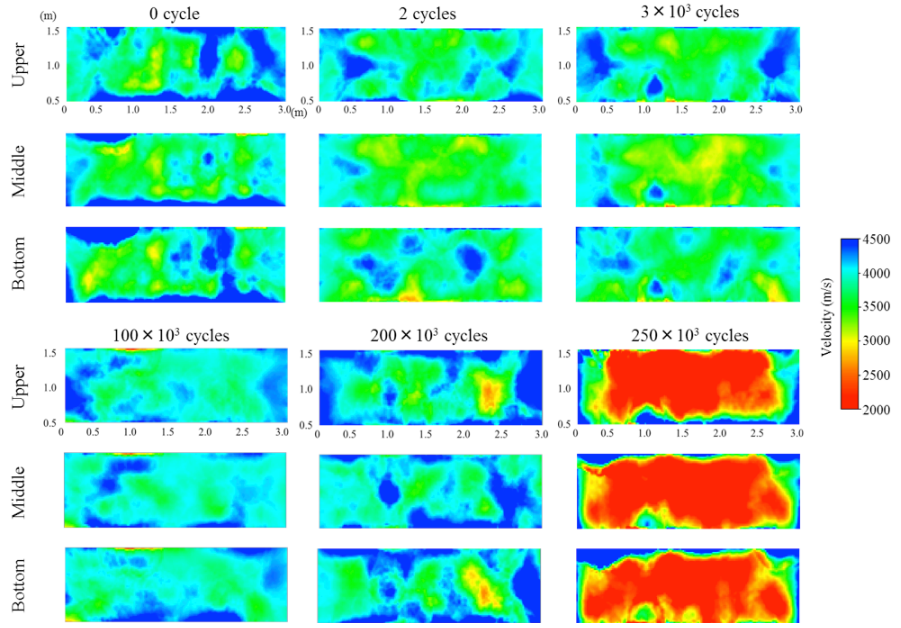

Figure 3. 3D velocity distributions of slab in each cycle under dry condition.

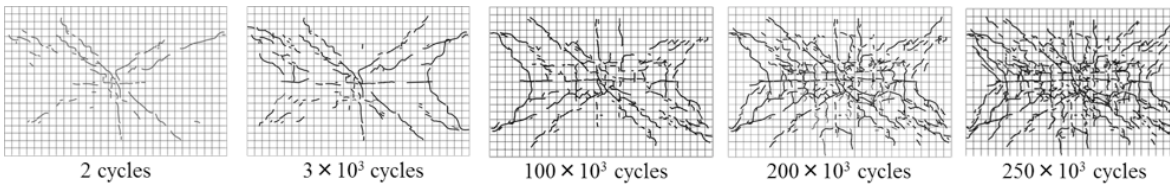

Figure 4. Crack evolution on the bottom.

3.2 Water charged condition

Velocity distributions based on three-dimensional elastic wave tomography are obtained before loading, after 100k and 200k load repetitions, and after the failure. The area of analysis is divided into 6 x 22 x 3 cells, while only the central area of 0.7 x 2.5 x 0.16 m as shown in Fig. 5 is focused. Reliable elastic wave signals which have DD-value [9] of more than 0.05 [10] are involved in the tomography analysis. Tomograms of each load steps are shown in Fig. 5. In the case before loading (see 0 cycles), areas of slightly small velocity of 3,300 m/s are obtained, whereas overall velocity exhibits 4,400m/s, and therefore the specimen is appeared to be intact at this moment. In the case of 100k cycles, the areas of small velocity less than 3,000 m/s become more distinctive and continuously emerged in the transversal direction, resulting in the average velocity of 4,000 m/s. In the case of 200k cycles, areas of small velocity less than 3,000 m/s widely evolve over the area of interest, and damage areas evaluated by the velocity less than 2,700 m/s, which is concluded by our past paper [6], are observed both in the middle and the bottom layers. As areas demonstrating large velocity of more than 4,000 m/s are still remained in places at this step, this appears to be the stage where damage and intact areas are mixed. At this stage the average velocity is 3,800 m/s. After the fatigue limit, further areas are damaged spreading widely over the area of interest. The damage is more obvious for the middle and the bottom layers than of the top layer; however, the average velocity is 3,700m/s, showing very small difference to the average velocity of 3800 m/s in the previous step. In consideration of the velocity decrease with steps as well as specific distributions of small velocity, it is implied that the damage is only generated at the specific areas.

In Fig. 6, crack traces overlaid with tomograms are exhibited for each case. Transversal cracks are developed firstly namely 100k cycles, then evolve in the same direction, and finally forming a cell like pattern. As for the tomograms, they are enlarged horizontally/ longitudinally from the each veridical/ transversal smaller velocity areas which is initially developed in 100k cycles. Note that the number of cycles (equivalent cycles of 98 kN loading) showing final fatigue limit is 17,025,097 in dry

condition and 8,654,440 in water filled condition i.e., in water filled condition the fatigue strength becomes a half of dry condition. This suggests that water infiltrating into the developed initial cracks, evidently enhance or accelerate the fatigue damage evolution. The transversal cracks and their lateral expansion as well as the same trend of tomograms accord well to this fact.

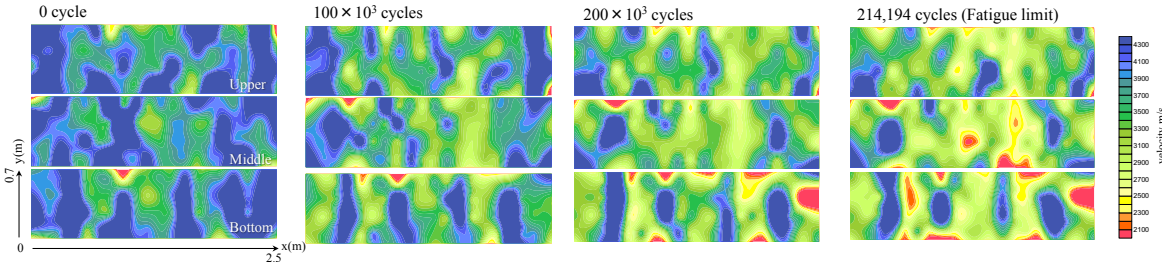

Figure 5. 3D velocity distributions of slab in the case allowing water infiltration.

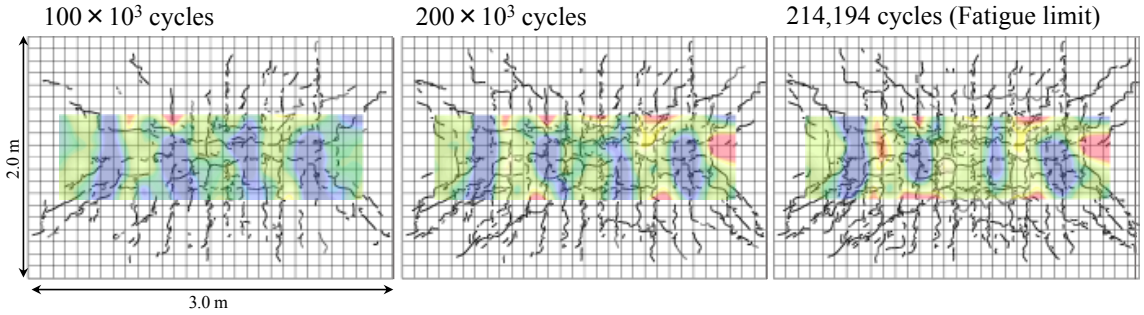

Figure 6. Crack traces on bottom surface overlaid with tomograms.

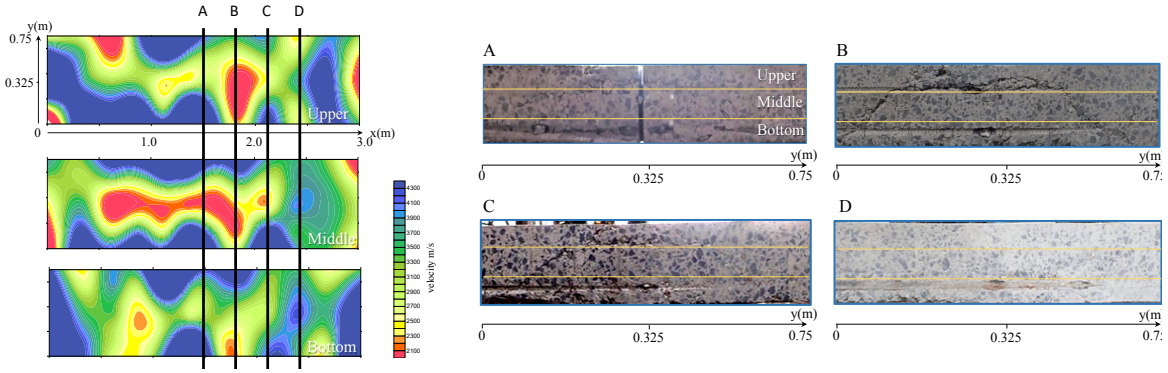

Figure 7. Tomograms combined with AE activity and sectional photos (A-D) after failure.

As shown in Fig. 5, the fatigue damage process can be reasonably evaluated by the tomograms, specifically for the middle and bottom layers; however, an expected aggregation area, which will be developed in the upper region at fatigue limit cycles, is not well assessed because the area beneath the load area have insufficient density of wave paths, and therefore AE sources obtained during the static load application are utilized in addition to the data derived by the elastic wave tomography. As in Fig. 7, different tomograms of upper and middle layers are obtained from those of only by the elastic wave tomography (see Fig. 5), suggesting the realistic result of tomogram in these areas. Although direct comparison with Fig. 5 cannot be carried out because of the difference of analytical resolution, the trend of small velocity in the bottom, developing transversal direction of damage is almost identical to that of Fig. 5. Hereafter transversal sections denoting A to D in Fig. 13 are focused with corresponding pictures to these sections as shown in Fig. 7 right. From Fig. 7, almost agreement is found between low velocity area and the corresponding area of damage by photos, e.g., in section B of Fig. 7 right, extraordinary aggregation can be observed in the boundary between the upper and middle layer, and moreover diagonally developed cracks heading to the bottom are distinctly observed. In addition, the cracks lay more in the left side namely 0-0.325 m in section B. Surprisingly these crack conditions accord pretty well to the concentrated damage areas evaluated by tomogram in section B of Fig. 7 left (see 0-0.325m in Y). Through the comparison between sectional observations

and corresponding tomograms, it can be concluded that the location of aggregation can be reasonably estimated by the velocity smaller than 2,300 m/s, which is obtained from the tomography with sufficient density of wave/ ray paths. For the in-situ bridge deck evaluation, when sufficient AE sources are obtained, spreading over the area of measurement, resulting in a reliable ray paths density, identification of aggregation can be implemented with the AE tomography.

5. Conclusions

In the paper, fracture processes of concrete decks are visualized by the acoustic approaches. Specifically, RC slabs with/ without water supply subject to wheel loads are cyclically damaged with monitoring acoustic approaches. As a result, depending on the water condition, different pattern of fracture progress can be confirmed from crack traces and tomograms. Specifically, overall spreading of cracks can be found in dry condition, whereas evolutional crack behavior from initial formed cracks can be assumed in water condition. In consideration of the fatigue limit for the both cases as well as tomograms, acceleration of fatigue failure is obvious in the case of water supply, and this might be implemented by the water existence causing tensional pressure in the formed cracks.

References

[1] The Ministry of Land, Infrastructure, Transport and Tourism: Annual report 2015 on maintenance of roads, Japan, (2015). (In Japanese).

[2] T. Shiotani, S. Yoshimi, T. Kamada, H. Ohnishi, S. Momoki and HK. Chai, "Visualization of fatigue damage for concrete bridge deck with stress wave techniques," *Structural Faults and Repair 2010*, CD-ROM, 2010.

[3] T. Shiotani, H. Ohtsu, S. Momoki, HK. Chai, H. Onishi and T. Kamada, "Damage evaluation for concrete bridge deck by means of stress wave techniques," *Journal of Bridge Engineering*, Vol. 17 (6), 847-856, 2012.

[4] T. Shiotani, T, N. Okude, S. Momoki and Y. Kobayashi, "Proposal of assessment method for infrastructures by AE tomography," *Proceedings of 2011 National Conference on Acoustic Emission*, 39-42, 2011 (in Japanese).

[5] Y. Kobayashi and T. Shiotani, "Seismic tomography with estimation of source location for concrete structure," *Structural Faults and Repair 2012*, CD-ROM, 2012.

[6] T. Shiotani, H. Asaue, T. Nishida, T. Maeshima and Y. Tanaka, "Evolution of fatigue damage in wheel-loading tests evaluated by 3D elastic-wave tomography," *Journal of Disaster Research* Vol.12(3), 487-495, 2017.

[7] Y. Tanaka, K. Maekawa, T. Maeshima, I. Iwaki, T. Nishida and T. Shiotani, "Data assimilation for fatigue life assessment of RC bridge decks coupled with path-integral-mechanistic model and non-destructive inspection," *Journal of Disaster Research* Vol.12(3), 422-431, 2017.

[8] Y. Kobayashi, T. Shiotani and H. Shiojiri: Damage identification using seismic travel time tomography on the basis of evolutional wave velocity distribution model, *Structural Faults and Repair 2006*, CD-ROM, 2006.

[9] J. Xu, "An effective way to validate signal arrival time in AE structural monitoring," *Advanced Materials Research*, Vols. 163-167, 2471-2476, 2010.

[10] H Asaue, H., T. Shiotani, K. Hashimoto and S. Kayano, "Development of AE monitoring system with accelerometers for in-situ RC slab," *Proceedings of 2017 National Conference on Acoustic Emission*, 25-28, 2017. (in Japanese)